(DRAFT) Mars Science Laboratory Entry Guidance Improvements for Mars 2018 (DRAFT)

Eduardo García-Llama
GBTech, Inc.
NASA/JSC/EG5
Houston, TX 77058
281-483-8223
eduardo.g.llama@nasa.gov

Richard G. Winski
Analytical Mechanics Associates
NASA/LaRC/D205
Hampton, VA, 23681
757-864-4116
richard.g.winski@nasa.gov

Jeremy D. Shidner
Analytical Mechanics Associates
NASA/LaRC/D205
Hampton, VA, 23681
757-864-4516
jeremy.d.shidner@nasa.gov

Mark C. Ivanov
JPL
Pasadena, CA 91109
888-888-8888
mark.c.ivanov@jpl.nasa.gov

Myron R. Grover
JPL
Pasadena, CA 91109
818-393-2478
myron.r.grover@jpl.nasa.gov

Ravi Prakash
JPL
Pasadena, CA 91109
888-888-8888
ravi.prakash@jpl.nasa.gov

Abstract— (DRAFT) In 2011, the Mars Science Laboratory (MSL) will be launched in a mission to deliver the largest and most capable rover to date to the surface of Mars. A follow on MSL-derived mission, referred to as Mars 2018, is planned for 2018. Mars 2018 goals include performance enhancements of the Entry, Descent and Landing over that of its predecessor MSL mission of 2011. This paper will discuss the main elements of the modified 2018 EDL preliminary design that will increase performance on the entry phase of the mission. In particular, these elements will increase the parachute deploy altitude to allow for more time margin during the subsequent descent and landing phases and reduce the delivery ellipse size at parachute deploy through modifications in the entry reference trajectory design, guidance trigger logic design, and the effect of additional navigation hardware.

TABLE OF CONTENTS

1. INTRODUCTION (DRAFT)

In 2011, the Mars Science Laboratory (MSL) will be launched in a mission to deliver the largest and most capable rover to date to the surface of Mars. A follow on MSL-derived mission, referred to as Mars 2018, is planned for 2018. Mars 2018 goals include performance enhancements of the Entry, Descent and Landing (EDL) over that of its predecessor

MSL mission of 2011. This paper will discuss the main elements of the modified 2018 EDL preliminary design that will increase performance on the entry phase of the mission. In particular, these elements will reduce the delivery ellipse size at parachute deploy and increase the parachute deploy altitude to allow for more time margin during the subsequent descent and landing phases.

To accomplish the goal of improved performance on entry, Mars 2018 will extend the limits of the entry technologies and entry guidance design qualified by MSL. This paper will show the main effects of specific new features of the entry design on the improved EDL performance such as the selection of a new entry vehicle's lift to drag ratio (L/D), modifications in the entry reference trajectory design, guidance trigger logic design, and the effect of additional navigation hardware.

In terms of the delivered altitude at parachute deploy, a trade with selected L/D and entry mass as inputs will show the potential benefit in altitude that could be reached at parachute deploy taking into account dip altitude and dynamic pressure considerations as well as constraints on guidance saturation and peak loads.

In terms of the ellipse size at parachute deploy, this paper will show improvement in reducing the ellipse size when the parachute deploy trigger is range-based rather than velocity-based as is the case in MSL. Besides the obvious gain in range accuracy, it will be shown how the dispersed Mach and altitudes at parachute deploy compared to those resulting from a velocity-based parachute deploy trigger. Also, the paper will show the improvement in ellipse size reduction when the range-based trigger is combined with a smaller attitude initialization error which can be obtained via adding a star tracker device that will determine the initial attitude of the vehicle prior to entry interface.

2. ENTRY GUIDANCE (DRAFT)

Mars 2018 will utilize, as in MSL, an offset center of mass to create a nominal angle of attack. This angle of attack generates lift which is used to reduce the landing error ellipse size and increase the parachute deploy altitude. Entry guidance provides bank angle commands throughout entry that orient the vehicle lift vector to compensate for dispersions in initial delivery state, atmospheric conditions, and aerodynamic performance. This enables the vehicle to
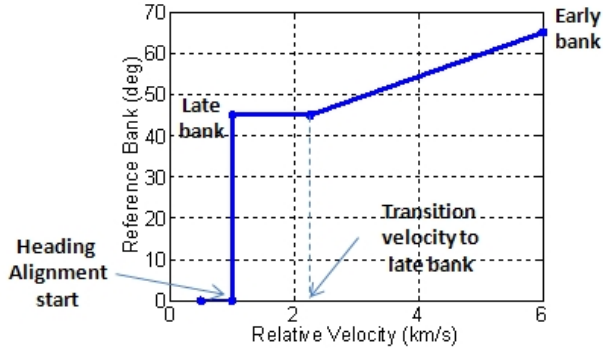
Figure 1. Reference profile definition.

arrive close to the desired state at parachute deployment.

The Mars 2018 will use an Apollo-derived entry guidance algorithm [1],[2]. The algorithm is divided into three phases. Entry interface marks the start of guided entry: guidance is initialized in the pre-bank phase and the controller commands bank attitude hold until the sensed acceleration exceeds 0.1 Earth g's. Once the sensed acceleration exceeds the specified trigger limit, the range control phase begins.

During the range control phase, the bank angle is commanded to minimize predicted downrange error at parachute deployment. Throughout this phase, crossrange error is maintained with a manageable deadband limit by executing bank reversals as necessary. Peak heating and peak deceleration occur during this guidance phase.

Once the navigated relative velocity drops below a certain value, guidance transitions to a heading alignment phase. During this phase, the guidance no longer controls downrange error. Instead, the guidance commands a bank angle to minimize residual crossrange error and azimuth error before parachute deployment. However, the bank angle during heading alignment is limited to ensure that a sufficient amount of lift is commanded to achieve the desired altitude performance.

Just prior to parachute deployment, the vehicle angle of attack is adjusted to 0° by ejecting balance masses while the azimuth is aligned for better radar performance later during parachute descent. Parachute deployment is triggered at a navigated velocity of over 450 m/s when a velocity trigger is used.

3. CONCEPTS (DRAFT)

Some concepts that will be used in different parts of the paper will be defined in this section.

Reference Trajectory Design Map

The reference trajectory design map consists of a parametric study used to determine the entry flight path angle and the shape of the reference profile that maximizes the parachute deploy altitude under certain conditions for each L/D and entry mass combination. The shape definition of the reference profile in terms of bank angle vs. relative velocity employs the same parameters that define the MSL reference profile (see Figure 1): an early bank angle at entry interface that linearly ramps down to a late bank angle that remains constant until the heading alignment velocity is reached.

The early and late bank angles, the transition velocity to late bank, the entry mass, the total L/D and the entry flight path angle of the vehicle are parameters of the reference trajectory design map. Once run under nominal conditions, the design map can be filtered to obtain the reference profile that results in the highest parachute deploy altitude under some specific conditions for each entry mass and total L/D combination.

Guidance Saturation

In a vehicle that modulates its vertical L/D using the bank angle only, the control response is said to saturate when the bank angle command results in the maximum or minimum vertical L/D. Maximum and minimum vertical L/D's happen when the bank angle is 0° and 180°, respectively.

Following the guideline that was set for MSL, guidance saturation is defined in this paper as the percentage of time during the entry phase that guidance is commanding a bank whose absolute value is within 15° away from saturation.

The guidance is not saturated when flying a trajectory under nominal conditions; it can be saturated when flying under dispersed conditions. Guidance saturation for a particular trajectory profile is assessed in worst case conditions in order to inform how the reference trajectory is expected to perform prior to its evaluation in a Monte Carlo simulation. Worst case conditions to assess guidance saturation defined for MSL account for a L/D that is 20% smaller than the nominal, an atmospheric density 15% larger than the nominal, a ballistic number 15% smaller than the nominal and an entry flight path angle 0.2° steeper than the nominal [7]. Under these stress conditions, the guidance will try to fly more lift-up in order to reach its target and, therefore, it will be more prone to saturate.

Altitude Dip Constraint

To achieve maximum altitude at parachute deploy, the trajectories tend to dive steeply in the atmosphere to rise up, or loft, at the end of the trajectory [3],[4]. In some cases, especially when the L/D's and ballistic numbers are high, the trajectories may tend to dive in too steeply, potentially reaching very low altitudes in the middle of the trajectory before gaining altitude again at the end. Those low altitudes are called herein dip altitudes and may be too low in some cases.

The dip altitude constraint is the minimum acceptable altitude in the middle of a trajectory in a nominal case. In selecting the dip altitude constraint, it is important to keep in mind what happens under dispersed conditions. Under dispersed conditions, the worst case dip altitude may be a few kilometers below the nominal dip altitude.

A 10 km dip constraint is selected in this study. This is the value that has traditionally been used for different final altitude maximization studies that have been carried out to date [3],[4]. In any case, the dip constraint of 10 km is an arbitrary value and therefore can be changed. The selected value depends on the acceptable minimum altitude for dispersed trajectories.

4. INCREASED DELIVERY ALTITUDE AT PARACHUTE DEPLOY (DRAFT)

In order to find the maximum altitude at parachute deploy that could be achieved for each possible L/D and entry mass combination, the reference trajectory design map was run.

Table 1. **Reference Trajectory Design Map**

Parameter	Range of values	Increment
L/D	0.24 - 0.36	0.01
Entry Mass (mt)	3 - 4.2	0.3
Entry Flight Path Angle (deg)	-13 to -19	0.5
Early Bank (deg)	55 - 135	10
Transition Velocity to Late Bank (km/s)	2 - 3	0.25

The ranges of values used in the design map in this paper for each of the parameters are shown in Table 1.

During the MSL's reference trajectory design process, it was learned that, for a given L/D and entry mass, the entry flight path angle and the early bank are the parameters that influence the most in the parachute deploy altitude. The late bank affects the parachute deploy altitude as well but it has a more significant influence in the ability of the guidance to accommodate dispersions at the end of the trajectory and thus to reduce the ellipse footprint at parachute deploy.

Since the conceptual design phase of MSL starting in 2000, reference trajectories usually had a 45° late bank. Lower late bank angles would result in higher parachute deploy altitudes as well as in larger ellipse footprints. Higher late banks would have the opposite effect. At this early stage in the design of the reference trajectory, a late bank of 45° has been selected because it offers a good compromise between parachute deploy altitude and ellipse size footprint.

The transition velocity to late bank has a small influence in the altitude at parachute deploy. MSL's transition velocity is often 2.0 km/s. In this paper, the possible range of values for this parameter was extended to 3 km/s. The entry velocity was selected to be 6 km/s. In all the cases, the heading alignment starts at 1 km/s, 0.1 km/s lower than in MSL. This difference has practically no effect in the parachute deploy altitude. Future refinements in the selection of these values should be expected.

With Guidance Saturation Constraint

Figure 2 shows the parachute deploy altitude contour lines as a function of L/D and entry mass resulting from the design map with the altitude being referenced to the Mars MOLA (Mars Orbiting Laser Altimeter) areoid surface definition [8]. The results from the design map have been filtered to find those that provide the highest parachute deploy altitude under the condition that the worst case guidance saturation is smaller than 20% (this is the design value used in MSL). This constraint improves the robustness of the entry guidance by ensuring sufficient vertical L/D is held in reserve to accommodate dispersions.

A 10 km dip constraint was originally added as a condition in the selection of the reference profile and entry flight path angle. When this constraint was used, only the cases with high entry mass and high L/D were affected. Later Monte Carlo simulations showed that the lowest dip altitudes were higher than 7 km in all the cases with the exception of the case with highest L/D (0.36) and highest entry mass (4.2 mt) which had a minimum dip altitude of about 6.5 km under dispersed
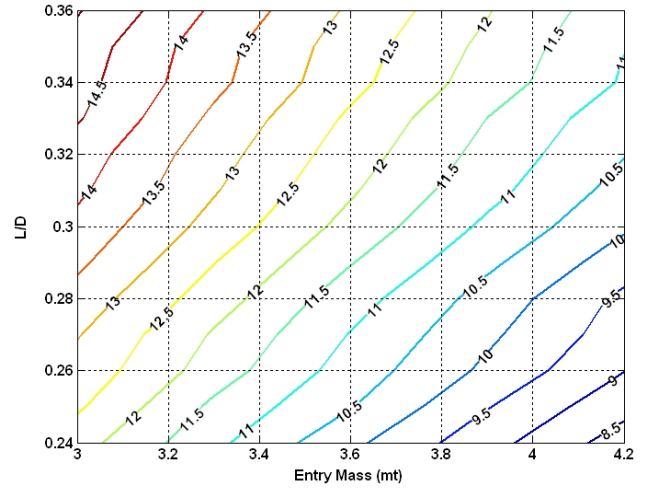

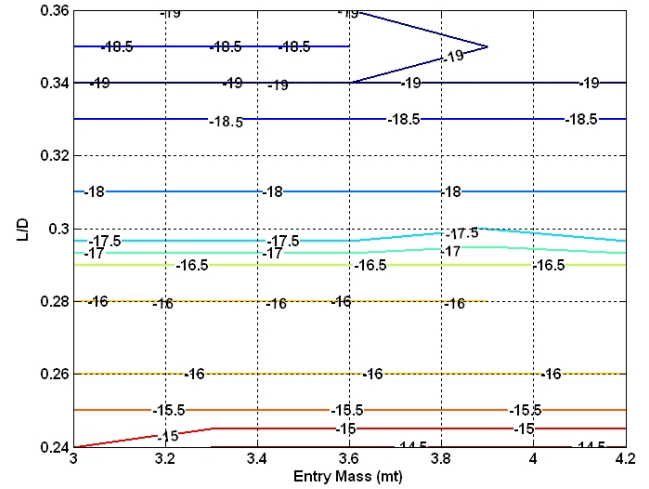**Figure 2**. Parachute deploy altitude (km).

Figure 3. Entry flight path angle (deg).

conditions. Given the fact that the worst case dip altitudes in the design map were still high, the altitude dip constraint was disregarded at this stage of the design. Therefore Figure 2 shows the parachute deploy altitude contour lines for the case in which the 10 km dip constraint was not used.

Each point in figure 2 is associated to a particular reference trajectory and entry flight path angle. Figures 3, 4 and 5 show the entry flight path angles, early banks and transition velocities of the reference trajectories associated to the results shown in Figure 2. Figures 3, 4 and 5 show that the parameters they present are, for the most part, independent of the entry mass. In addition, Figure 5 shows large areas with transition velocities equal to 3 km/s. Because 3 km/s is the upper limit value used in the design map, this trend indicates that higher parachute deploy altitudes could be expected should the transition velocity to late bank be enlarged in the design map. In any case, this possibility was not explored further in this paper.

Figure 2 constitutes a useful tool in the design process because it shows how much L/D is required in order to obtain a desired parachute deploy altitude for a given entry mass. Appendix A shows the partial derivatives for all L/D and entry mass combinations.
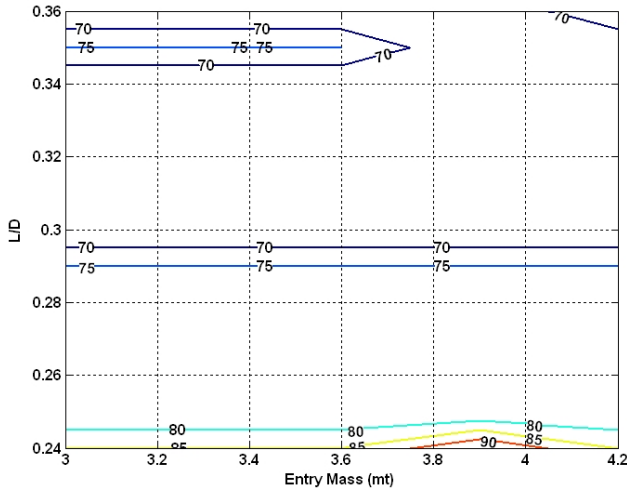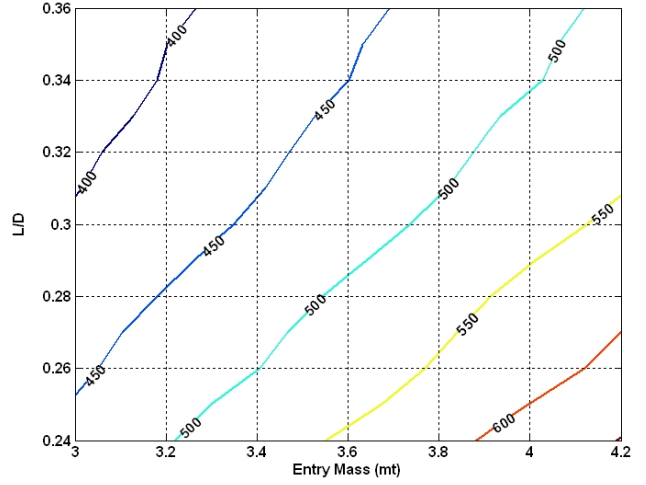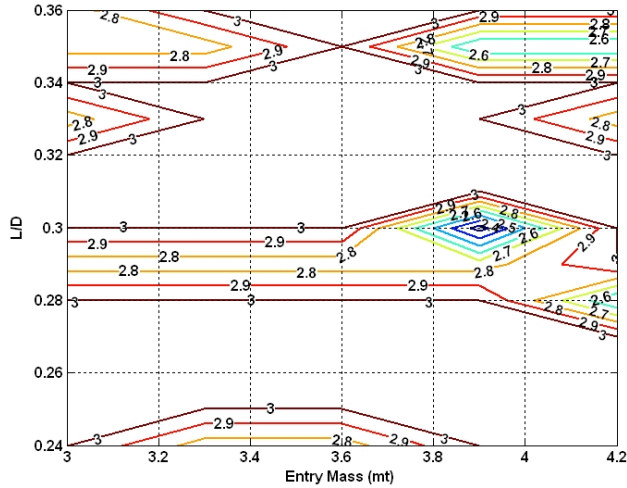
3

Figure 4. Early bank (deg).

Figure 5. Transition velocity to late bank (km/s).

Figure 6. Dynamic Pressure (Pa).
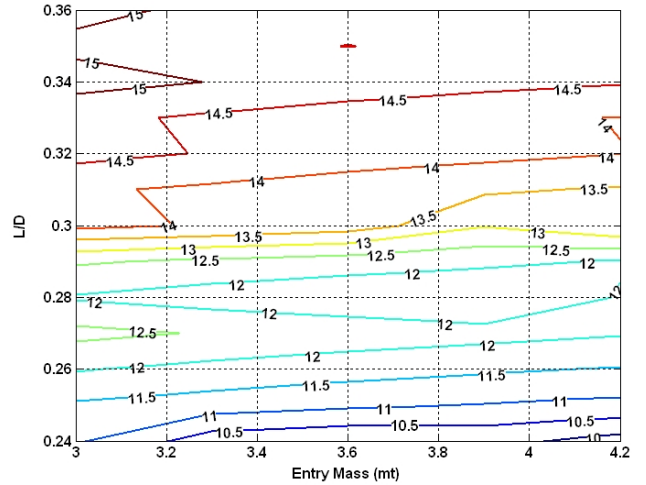

Figure 7. Maximum load (g's).

Figure 8. Parachute deploy altitude (km).

Figure 6 shows the dynamic pressure at parachute deploy. It can be observed that the dynamic pressures are well within the MSL's parachute deploy qualification limit of 850 Pa [9].

With the Addition of Peak Load Constraint

MSL entry vehicle structure is designed for 15g peak loads during entry. During the design of MSL's entry guidance it was observed that if the nominal trajectory had a peak load smaller than 13g then the dispersed peak loads would remain below 15g. When the design map is not filtered with the 13g peak constraint, the cases with L/D higher than 0.3 surpass that value with a maximum at about 15g as it is shown in Figure 7.

Assuming that Mars 2018 will have the same entry vehicle structural limit, and because the range control logic in the entry guidance is not explicitly commanding to limit acceleration loads, the design map was additionally filtered to result only in cases with a peak load of 13g.

Figure 8 shows how the parachute deploy altitude contour lines get modified when the 13g peak load constraint is applied to the design map. Appendix B shows the partial derivatives for all L/D and entry mass combinations when the
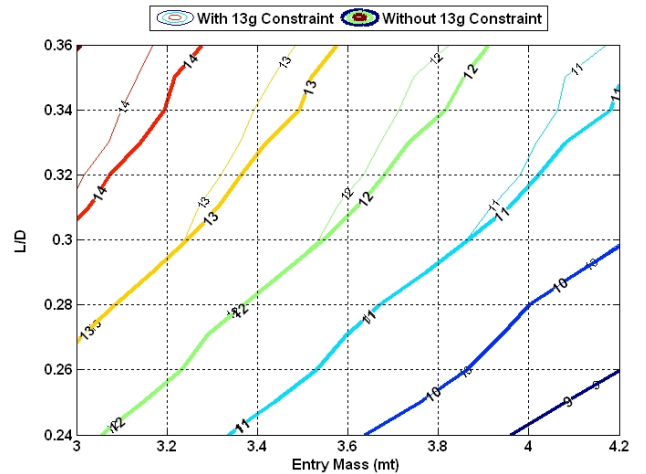
4

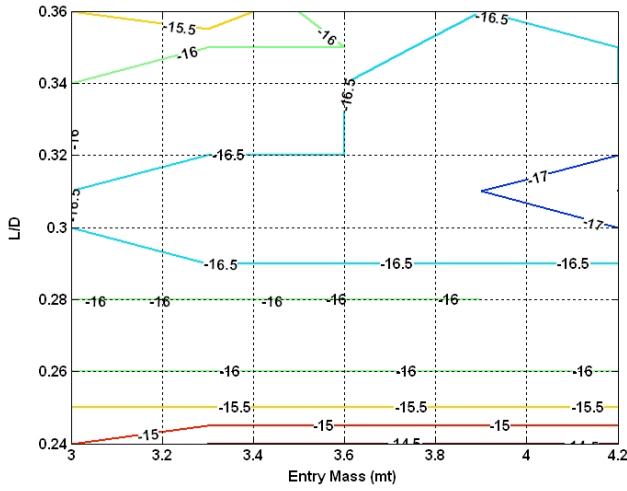**Figure 9**. Entry flight path angle (deg).

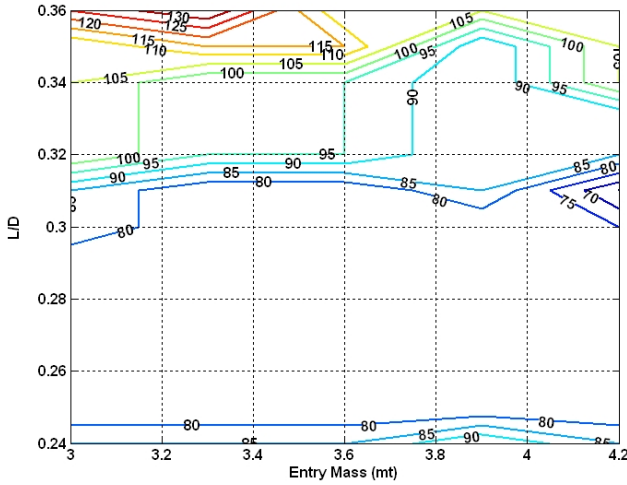**Figure 11**. Transition velocity to late bank (km/s).

Figure 10. Early bank (deg).

peak load constraint is combined with the guidance saturation constraint.

Figures 9, 10 and 11 showing the entry flight path angles, early banks and transition velocities associated to the altitude contours with 13g constraint are included for reference.

5. ELLIPSE SIZE REDUCTION AT PARACHUTE DEPLOY (DRAFT)

The dispersed ellipse size at parachute deploy is driven by three factors. One is the navigated position knowledge error as the guidance cannot reduce the ellipse size any smaller. Another factor is the residual downrange error that results from a velocity-based parachute deploy trigger, although in MSL this contribution was secondary to the knowledge error magnitude. Third, the guidance accuracy is sensitive to the attitude initialization error prior to cruise stage separation [5]. This section will show the improvement in reducing the ellipse size at parachute deploy when the deploy trigger is range-based rather than velocity-based and when a smaller attitude initialization error is used. In this section, since a L/D and entry mass has not yet been selected for Mars 2018, the MSL's L/D and entry mass will be selected for comparison
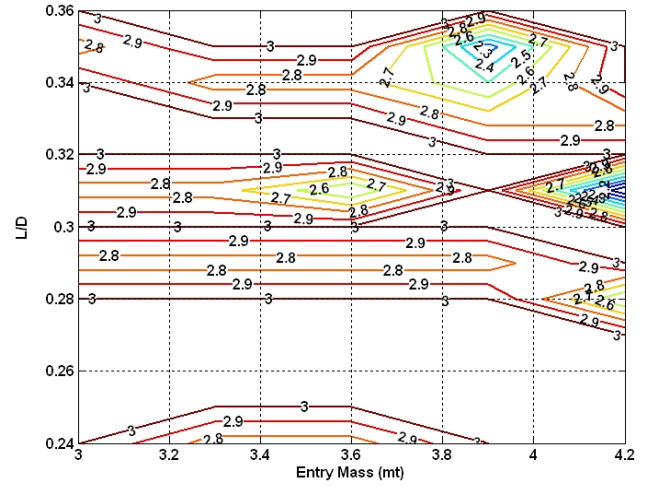
purposes (the entry mass will be the one used in the design map that has the closest value to the MSL's entry mass). The reference trajectory that will be used in this section is that which corresponds to a L/D = 0.24 and an entry mass = 3.3 mt in Figure 2: -14.5° entry flight path angle, 85° early bank, 45° late bank, 2.75 km/s transition velocity to late bank and 1.0 km/s transition velocity to heading alignment (for reference, since the conceptual design phase of MSL starting in 2000, reference trajectories usually had near -15.5° entry flight path angle, 65° early bank, and 45° late bank angle. The velocities of the ramp between early and late bank have varied but the reference late bank angle is often achieved at 2 km/s).

Monte Carlo Products (This section is not complete yet)

The following subsections will show Monte Carlo results. The characteristics of the Monte Carlo simulations, the dispersions used, and the statistics used for the evaluation of the data will be discussed in this subsection.

Monte Carlo runs are conducted with 8,000 randomly perturbed cases in addition to the nominal. Experience has shown this number to be a reasonable balance between statistical accuracy and computer run time. Traditionally, in the MSL project, performance metrics have been tracked by a 0.13 percentile or 99.87 percentile statistics. This convention is used to provide requirements with a high probability (3-sigma percentile under the assumption of a Gaussian distribution) of success that is insensitive to the underlying distribution or the number of cases run [5]. Continuing with this practice, performance metrics will be tracked by the same convention in this paper.

Range Trigger Versus Velocity Trigger for Parachute Deploy

In Reference [6], a side-by-side comparison of parachute deployment triggers was conducted for MSL. Two triggers, the baseline velocity trigger and an alternate range trigger, were tuned to produce the same nominal parachute deploy Mach number. For each trigger a 6-DoF (Degree of Freedom) Monte Carlo analysis of 8,000 runs was performed using the MSL POST2 (Program to Optimize Simulated Trajectories II) end-to-end EDL performance simulation. The results of this study showed that a range trigger has the potential to significantly reduce footprint size with negligible Mach increase and no altitude loss.
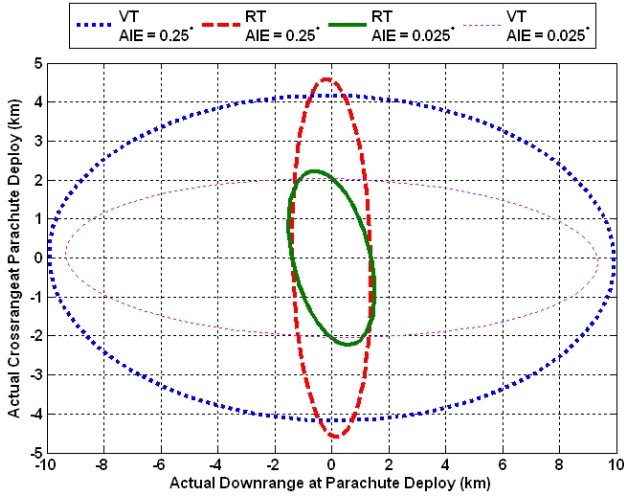
Figure 12. 99.87%-tile Ellipse footprint at parachute deploy (VT = Velocity Trigger, RT = Range Trigger, AIE = Attitude Initialization Error).

Figure 13. 99.87%-tile Altitude over the Mars MOLA areoid vs. Mach number at parachute deploy (VT = Velocity Trigger, RT = Range Trigger, AIE = Attitude Initialization Error).

The same type of Monte Carlo comparison was performed using the proposed new reference profile. The results show the same trend as that presented in Reference [6] in terms of the significant reduction in the ellipse size footprint when the range trigger is used. Figure 12 shows thecomparison of the ellipse footprint for the velocity trigger and the range trigger when the attitude initialization error of 0.25° is used (Figure 12 also shows the ellipse footprint for the case when the range trigger with an attitude initialization error of 0.025° is used. This case will be discussed in the next section. Figure 12 also includes the velocity trigger case with an attitude initialization error of 0.025° for reference).

Figure 13 shows the results for the altitude vs. Mach number at parachute deploy where the altitude is referenced to the Mars MOLA areoid surface definition. Figure 13 shows that there is not a significant difference in performance between the velocity trigger case and the range trigger case when an attitude initialization error of 0.25° is used (Figure 13 also shows the ellipse for the case when the range trigger with an attitude initialization error of 0.025° is used. This case will be discussed in the next section. Figure 13 also includes the velocity trigger case with an attitude initialization error of 0.025° for reference).

Figure 14 showing the dynamic pressure vs. Mach at parachute deploy is included for reference.

Attitude Initialization Error Prior to Entry

The attitude initialization error (IMU misalignment at the last navigation upload prior to entry) results in velocity and position knowledge errors perpendicular to the direction of deceleration during entry. This results in crossrange and altitude position knowledge errors. More importantly, it also results in altitude rate estimation errors which directly impacts the entry guidance predicted range errors because the altitude rate is a quantity used by the guidance to predict the range flown. Greater attitude initialization errors result in greater range deploy errors. Sufficiently large attitude initialization errors will dominate over other factors in the ellipse size [7].

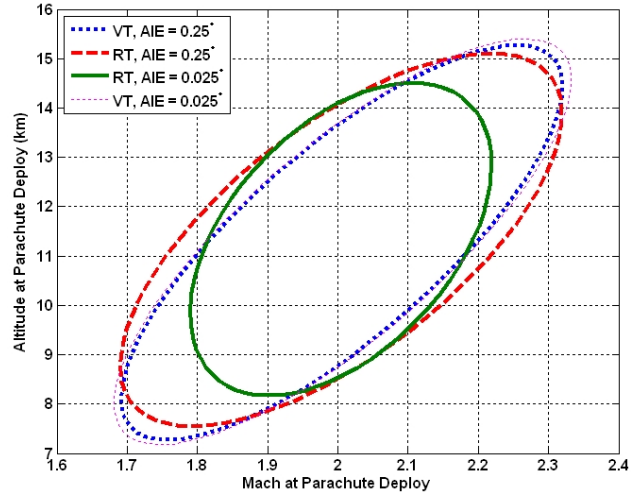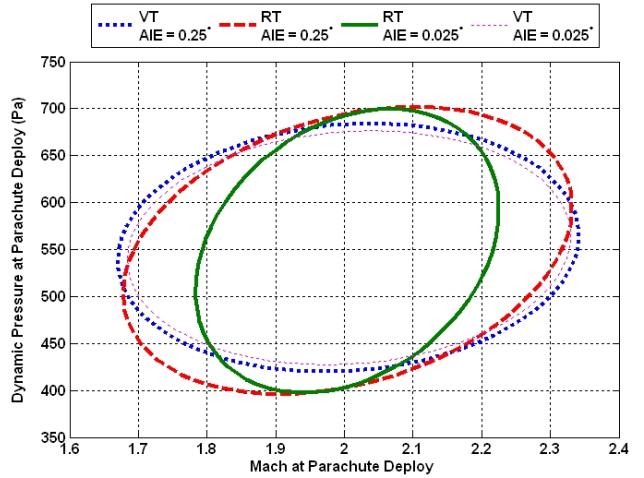MSL has a maximum attitude knowledge initialization error

Figure 14. 99.87%-tile Dynamic pressure vs. Mach number at parachute deploy (VT = Velocity Trigger, RT = Range Trigger, AIE = Attitude Initialization Error).

of 0.25°. The goal for Mars 2018 is to have this error reduced as much as possible through the addition of a star tracker in the entry vehicle that will determine the vehicle's attitude prior to entry. A specific star tracker model to carry out this operation has not been selected yet, however, low cost and all purpose star trackers for space applications can typically provide accuracies of about 20 arc-seconds (high precision star trackers can be found capable of determining the attitude better than 1 arc-second) [10] [11]. In this paper, a conservative attitude knowledge error of 90 arc-seconds, which is a tenth of MSL's attitude initialization error (0.025°), is considered.

Figure 12 shows the improvement in ellipse size reduction when a range trigger with an attitude initialization error of 0.025° is used: the size of the ellipse footprint in this case is 4.7 km by 2.6 km in size; that is almost 13.4 times smaller than that corresponding to the current baseline (velocity trigger with attitude initialization error of 0.25°). In terms of altitude vs. Mach performance at parachute deploy, Figure 13 shows a more confined distribution of points in the range

trigger case with attitude initialization error of 0.025°: the 99.87%-tile ellipse size in this case is almost 20% smaller than that corresponding to the velocity trigger case with an attitude initialization error of 0.25°. The results also show that the minimum deploy altitude is raised about one kilometer and that the maximum Mach is reduced by about 0.1 when the range trigger with attitude initialization of 0.025° is used.

6. SUMMARY (DRAFT)

The paper shows the main effects of specific new features of the Mars 2018 mission that will result in improved EDL performance over the current MSL mission.

The entry flight path angles and reference trajectories that result in maximum parachute deploy altitude have been found for a set of different L/D and entry mass combinations, taking into account dip altitude and dynamic pressure considerations as well as constraints on guidance saturation and peak loads. These results constitute a useful tool in the design process because they show how much L/D is required in order to obtain a desired parachute deploy altitude for a given entry mass.

A comparison in performance between a range-based trigger and a velocity-based trigger for parachute deploy has been presented. The results show that the use of a range trigger barely affects the altitude vs. Mach distribution at parachute deploy while significantly reducing the ellipse size with respect to that of MSL.

The paper also shows the effect of a significant reduction in the attitude initialization error when it is combined with a range-based trigger for parachute deploy. The reduction in attitude initialization error is assumed to be achieved via adding a star tracker device that can determine the initial attitude of the vehicle prior to entry interface. The paper shows that for a conservative attitude initialization error of 0.025° (90 arc-seconds), equivalent to a tenth of the attitude initialization error in MSL, the resulting ellipse size at parachute deploy is 4.7 km by 2.6 km which is 13.4 times smaller than that corresponding to the MSL baseline. The results also show that the minimum deploy altitude is raised about one kilometer and that the maximum Mach is reduced by about 0.1 when the range trigger with attitude initialization of 0.025° is used.

APPENDICES
A. PARTIAL DERIVATIVES WITH GUIDANCE SATURATION CONSTRAINT

The shape of the altitude at parachute deploy as a function of L/D and entry mass in 3D can be decomposed into small planes as depicted in Figure 15.

Each of the planes in Figure 15 is defined by its normal unit vector $(n_{m_e}, n_{L/D}, n_h)$ and the point it is associated to $(m_{e_0}, L/D_0, h_0)$. The equation defining each plane is given by

$$ h = \frac{n_{m_e}}{n_h} (m_{e_0} - m_e) + \frac{n_{L/D}}{n_h} (L/D_0 - L/D) + h_0 \quad (1) $$
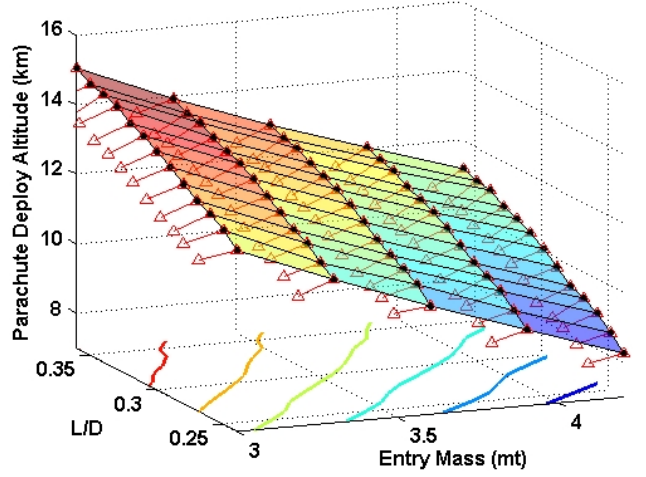

Figure 15. Normal vectors to parachute deploy altitude surface.

From Equation 1, the different partial derivatives can be calculated. The change in altitude with L/D is then given by

$$ \frac{\partial h}{\partial L/D} = -\frac{n_{L/D}}{n_h} \quad (2) $$

Similarly, the change in altitude with entry mass is given by

$$ \frac{\partial h}{\partial m_e} = -\frac{n_{m_e}}{n_h} \quad (3) $$

whereas the change in L/D with entry mass required to keep a constant deploy altitude is given by

$$ \frac{\partial L/D}{\partial m_e} = \frac{n_{m_e}}{n_{L/D}} \quad (4) $$

The partial derivatives when only the guidance saturation constraint is considered are presented in Figures 16 to 18 for each L/D and entry mass combination. Figure 16 shows the change in gained altitude at parachute deploy (expressed in km) for a change of 0.02 in L/D, Figure 17 shows the change in altitude for an increase of 0.3 mt in entry mass, and Figure 18 shows the increase in L/D required to keep a constant deploy altitude when there is an increase in entry mass of 0.3 mt.

B. PARTIAL DERIVATIVES WITH ADDITIONAL PEAK LOAD CONSTRAINT

Following the same procedure described in Appendix A, the partial derivatives for all L/D and entry mass combinations when the peak load constraint is combined with the guidance saturation constraint were found. Figure 19 shows the change in gained altitude at parachute deploy (expressed in km) for a change of 0.02 in L/D, Figure 20 shows the change in altitude for an increase of 0.3 mt in entry mass, and Figure 21 shows the increase in L/D required to keep a constant deploy altitude when there is an increase in entry mass of 0.3 mt.
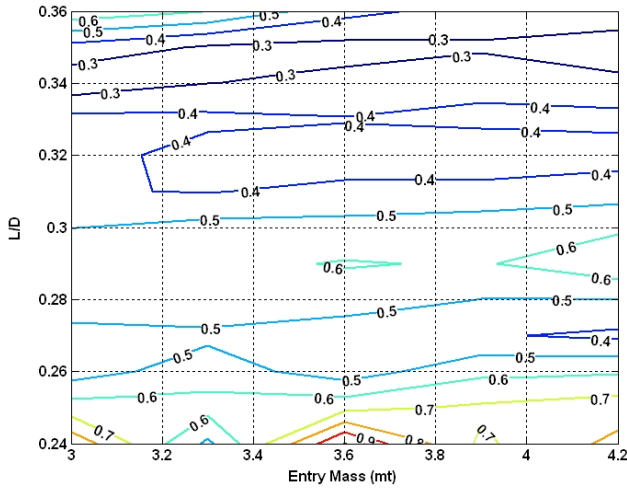
Figure 16. Gained altitude at parachute deploy (expressed in km) for a change of 0.02 in L/D with guidance saturation constraint.
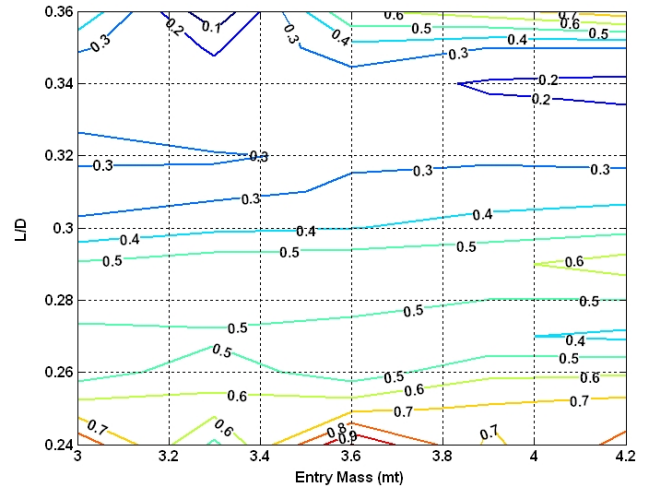

Figure 19. Gained altitude at parachute deploy (expressed in km) for a change of 0.02 in L/D with additional peak load constraint.
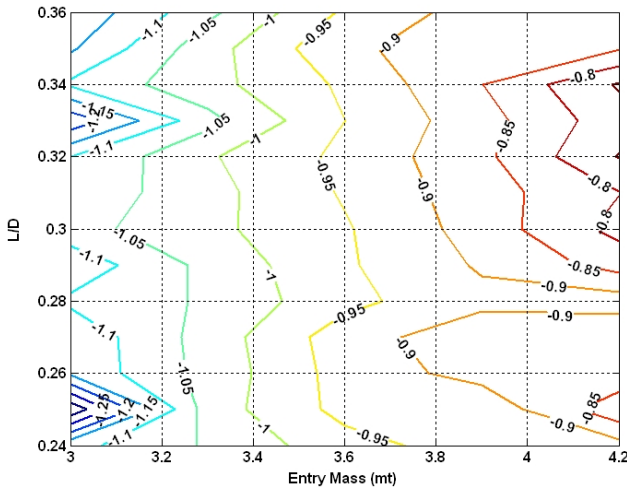

Figure 17. Gained altitude at parachute deploy (expressed in km) for a change of 0.3 mt in entry mass with guidance saturation constraint.
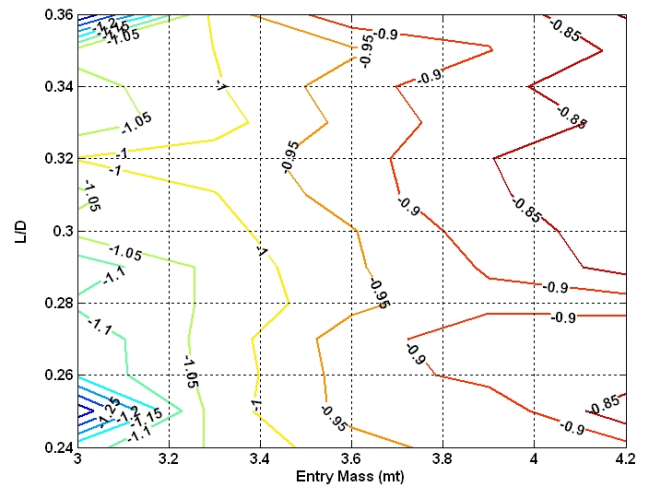

Figure 20. Gained altitude at parachute deploy (expressed in km) for a change of 0.3 mt in entry mass with additional peak load constraint.
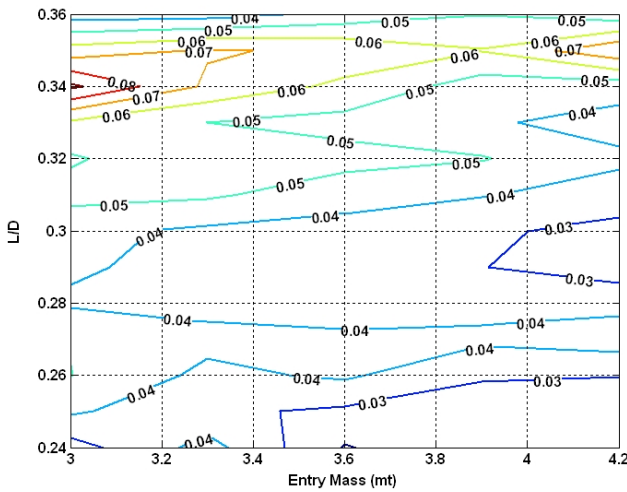

Figure 18. Required increase in L/D for an increase of 0.3 mt to keep a constant deploy altitude with guidance saturation constraint.
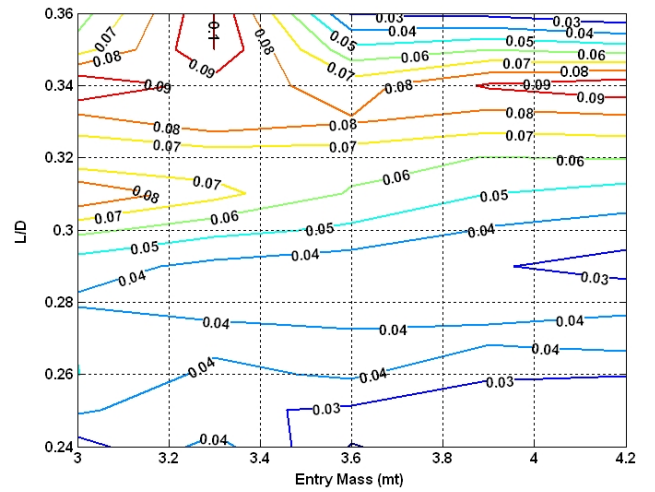

Figure 21. Required increase in L/D for an increase of 0.3 mt to keep a constant deploy altitude with additional peak load constraint.

8

In Figure 21, the plotted increase in L/D has been capped at 0.1 to ease visualization. In reality, values larger than 0.1 are associated to the region showing a L/D increase of 0.1.

ACKNOWLEDGMENTS

REFERENCES

[1] H.R. Morth, "Reentry Guidance for Apollo," MIT Instrumentation Lab., R-532, Vol. 1, Cambridge, January 1966.

[2] P.E. Moseley, "The Apollo Entry Guidance: A Review of the Mathematical Development and Its Operational Characteristics", TRW Note No. 69-FMT-791, TRW, December 1, 1969.

[3] J.M. Lafleur and C.J. Cerimele, "Angle of Attack Modulation for Mars Entry Terminal State Optimization." AIAA 2009-5611. AIAA Atmospheric Flight Mechanics Conference and Exhibit, Chicago, Illinois, 10-13 August 2009.

[4] J.M. Lafleur and C.J. Cerimele, "Mars Entry Bank Profile Design for Terminal State Optimization." AIAA 2008-6213. AIAA Atmospheric Flight Mechanics Conference and Exhibit, Honolulu, Hawaii, Aug. 18-21, 2008.

[5] R. Prakash, et al. "Mars Science Laboratory Entry, Descent, and Landing System Overview," 2008 IEEE Aerospace Conference Proceedings, March 1-8, 2008.

[6] D. Way, "On the Use of a Range Trigger for the Mars Science Laboratory Entry, Descent, and Landing", 2011 IEEE Aerospace Conference Proceedings, March 5-12, 2011.

[7] G.F. Mendeck and L.E. Craig, "Entry Guidance for the 2011 Mars Science Laboratory Mission." AIAA 2011-6639. AIAA Atmospheric Flight Mechanics Conference and Exhibit, Portland, Oregon, Aug. 8-11, 2011.

[8] M.T.Zuber, et al. "Mars Observer Laser Altimeter Investigation", Journal of Geophysical Research, Vol. 97, pp. 7781-7797, May 1992.

[9] D. Kipp, et al. "Mars Science Laboratory Entry, Descent, and Landing Triggers," 2007 IEEE Aerospace Conference Proceedings, March 3-10, 2007.

[10] C. Liebe, "Star Trackers for Attitude Determination", Aerospace and Electronic Systems Magazine, IEEE, Vol. 10, Issue 6, pp. 10 - 16, June, 1995.

[11] C. Liebe, "Accuracy Performance of Star Trackers - a Tutorial", IEEE Transactions on Aerospace and Electronic Systems, Vol. 38, Issue 2, pp. 587 - 599, April, 2002.